

**Green synthesis of Iron nanoparticle from the extract of waste cauliflower leaves: An application for the removal of an anionic dye (Methyl Orange)****Shalu Rawat, Pallavi Vishnoi and Jiwan Singh***

Department of Environmental Science, Babasaheb Bhimrao Ambedkar University, Lucknow, Uttar Pradesh, INDIA

*Received: 05 Dec 2019; Revised: 21 Jan 2020; Accepted: 25 Feb 2020***ABSTRACT**

In this study, we have synthesized iron nanoparticles with the help of an environmentally benign technique using the extract of waste cauliflower leaves (Ca-INPs). This method of green synthesis of nanoparticles reduces the hazardous impact chemical synthesis method as well as it also allows the use of biological waste for the synthesis that ultimately reduces the production cost. Synthesized were used for the adsorptive removal of an anionic dye Methyl Orange (MO) from its aqueous solution after characterizing them with scanning electron microscope (SEM) and energy dispersive spectroscopy (EDS). The adsorption process was optimized by varying different parameters that were Ca-INPs concentration, initial MO concentration, contact time and pH. Maximum adsorption of MO was found at 2 g/L concentration of MO with initial MO concentration 5 mg/L. equilibrium time for adsorption was observed to be 120 min. the adsorption process was also analyzed by the application of Langmuir and Freundlich isotherm and pseudo-first-order and pseudo-second-order kinetic to understand the mechanism behind the adsorption of MO onto Ca-INPs. The adsorption process was best followed by Freundlich isotherm and pseudo-second-order kinetic reaction. Maximum adsorption capacity of Ca-INPs for MO adsorption was found to be 21.73 mg/g.

Key words: Green synthesis; adsorption; nanoparticles; adsorption isotherm; adsorption kinetics**1) INTRODUCTION**

An extensive industrialization has brought the nature under extreme threat of pollution, availability of pure water and sustainable water treatment technology is one of the most concerned matters these days [1]. Effluent of industries like textile, pharmaceuticals, tanning, ceramics, paper and pulp etc. contain a heavy load of organic as well as inorganic pollutants are the major source of pollution in water bodies [2]. Artificial dyes are one of the most common pollutant in water and it can be easily detected as it is visible and highly undesirable [3]. According to an estimation production of synthetic dye annually is more than 700,000 tons annually globally [4]. Release of synthetic dyes into water is a serious matter of concern, many of these dye are reported to be potential carcinogenic and mutagenic in nature [5]. Beside this coloration of natural water by dyes also interrupts the process of photosynthesis in the water system and in this way disturbs the biological activities of a water body additionally it also degrades the aesthetic value of the water body [6]. Most of the synthetic dyes have complex molecular structure especially those with aromatic rings are stable to light, heat and natural biodegradation process, hence they persist in water for a long period of time [7]. Methyl Orange an acidic azo dye, frequently used in textiles industries, laboratories and some other commercial application. It is recalcitrant and toxic in

nature, known of causing vomiting, cyanopsis, tissue necrosis, increase in heart rate and shock [8]. Furthermore, removal of MO from effluent is difficult due to protonation behavior which depends on the pH of the medium [9]. Methods like, ion exchange, chemical oxidation/precipitation, photocatalysis and adsorption are some conventional techniques used for the removal of dyes from a water stream. Adsorption is among the sustainable technology that is acceptable due to its ease in operation, comparatively less cost input, less required management and high efficiency [10][11]. Although the versatility and cost of the adsorption process greatly depends on the adsorbent, the adsorbent should be highly efficient, recyclable and economically feasible for the successful enforcement of adsorption technology on a wide level [12].

Nanoparticles have good efficiency of adsorption due to their high surface to volume ratio, specific properties, large number of active sites and higher recycling ability [13]. In adsorption nanoparticles are highly effective due to their high surface to volume ratio and their capability to get modified by various processes for more efficiency [14]. Biological synthesis of nanoparticles using plant extract is an economically viable technique and it also lessen the

* Corresponding Author: **Dr. Jiwan Singh**
Email address: jiwansingh95@gmail.com

harmful environmental impacts of hazardous and toxic chemicals used in conventional chemical methods. These days' biological waste materials (vegetable waste or agricultural waste) are in focus for the nanoparticle synthesis that further decrease the cost of nanoparticle synthesis for example synthesis of silver nanoparticles using bilberry and red currant waste [15] and sapota fruit waste [16]. Similarly other metallic nanoparticles are also been synthesized using bio waste like red peanut skin for iron nanoparticles [17], onion peel for copper nanoparticles [18] and banana corn for zinc oxide nanoparticles [19]. India is a subtropical country a lot of wet organic waste is generated here on daily basis but there are not sufficient management techniques to cope with this mess, some portion of that waste organic matter is used in cattle feeding but rest of the waste is dumped here and there that create an environmental nuisance. On the other hand this waste is now being used for adsorbent preparation as they are rich in phytochemicals they are extensively now explored for the nanoparticle synthesis.

In this study we have used waste cauliflower leaves were used for the synthesis of iron nanoparticles, which were then used for the adsorptive removal of methyl orange dye from its aqueous solution. The process of adsorption was optimized by varying different physic-chemical parameters, the adsorption isotherm and kinetic were also studied.

2) MATERIALS AND METHODS

2.1 Materials

Methyl orange dye ($C_{14}H_{14}N_3NaO_3S$), Ferric chloride anhydrous ($FeCl_3$), NaOH and other chemical used in this study were supplied by Thermo-Fisher Scientific and all of them were of analytical grade. Preparation stock and working solution of MO were prepared in Millipore deionized water. The raw material for extract preparation that were, waste cauliflowers were collected from the local market.

2.2 Synthesis of iron nanoparticles

Collected leaves were washed with tap water and then with distilled water to remove all kind of impurities from the leave then they were dried in air for 2-3 days. The dried leaves were cut into small pieces and a 10 g of that was and mixed in 100 mL distilled water. The mixture was then heated on water bath at 90°C for 30 min in a beaker. After that the mixture was cooled and filtered the liquid part containing various phytochemicals was used for nanoparticles synthesis. Synthesis of nanoparticles was done by method of Lingamdinne et al. [20], with some modification. The leaf extract was then mixed in the $FeCl_3$ solution drop by drop, the color of the solution suddenly started to get change in intense black which showed the reduction of Fe^{+3} into Fe^0 . The solution was further stirred vigorously for two hours for homogenization of particle and then it was centrifuged at 10,000 RPM for 10 min. for the separation of nanoparticles from the suspension, the nanoparticle pellets were washed several times with distilled water followed by washing with ethanol the nanoparticles were then dried, characterized by SEM and EDS using JSM-6490 LV, JEOL, Japan model and then used for the adsorption of MO dye.

2.3 Adsorption experiment of MO dye

All the adsorption experiments were performed in the Erlenmeyer flask. For adsorption a 50 mL aqueous solution of MO (5 mg/L) was taken in the flask and a known amount of synthesized iron nanoparticles was added to it then it was shook in orbital shaker at 100 RPM for 240 min at 25°C and pH 7, after which the flask was taken out of the shaker and iron nanoparticles were separated by centrifugation and residual concentration of MO in the supernatant was determined by analyzing it with UV-Visible spectrophotometer (Systronics 117) at 464 nm wavelength. The percentage adsorption of the dye and its amount loaded on the unit mass of nanoparticle (q_t) was calculated by using the equation (1) and (2), respectively:

$$\% \text{ Adsorption} = \frac{C_i - C_t}{C_i} \times 100 \quad (1)$$

$$q_t = \frac{C_i - C_t \times V}{m} \quad (2)$$

Where, C_i denotes initial concentration of MO (mg/L) and C_t denotes concentration of MO after adsorption (mg/L), V is volume of the solution treated (l) and m represents the amount of nanoparticles used (g).

In order to find the optimum condition for the adsorption of MO various parameters were altered and this was done by altering one parameter at a time while keeping other constant. The parameters which were varied were concentration of iron nanoparticles from 0.1 g/L to 4 g/L, concentration of MO from 2.5 mg/L to 20 mg/L, contact time between adsorbent and adsorbate (from 5 min to 300 min), pH (4,6 and 10) and temperature (25 to 55°C).

3) RESULTS AND DISCUSSION

3.1 SEM and EDS analysis of the Ca-FeNPs

Results of the SEM and EDS analysis are shown in the Fig. 1 which represents that the synthesized iron nanoparticles are clumped together that resulted in the enhancement of particle size. Previous studies have documented that due to high surface free energy nanoparticles tends to clump together in order to neutralize that free energy. Larger size of nanoparticle may also result due to higher concentration of polyphenols in the cauliflower leaf extract that are responsible for reduction and capping of nanoparticles or due to pH alteration during synthesis of nanoparticles [21]. The EDS image shows peaks of three elements only Fe, Cl and O (Fig. 1c).

3.2 Effect of Ca-FeNPs concentration

Concentration of nanoparticle is an essential parameter in adsorption to be optimized as it is directly proportional to the number of active adsorption site to bind the adsorbate. On increasing the concentration of nanoparticles, number of active sites also increases that facilitates more interaction between adsorbent and adsorbate [22]. The nanoparticle concentration was varied in the range of 0.1 g/L to 4 g/L and the results are represented in Fig. 2b on increasing nanoparticle concentration from 0.1 to 2 g/L the adsorption percentage increased from 50 to 80% while the q_t value of nanoparticle decreased from 3.2 to 2.2 mg/g.

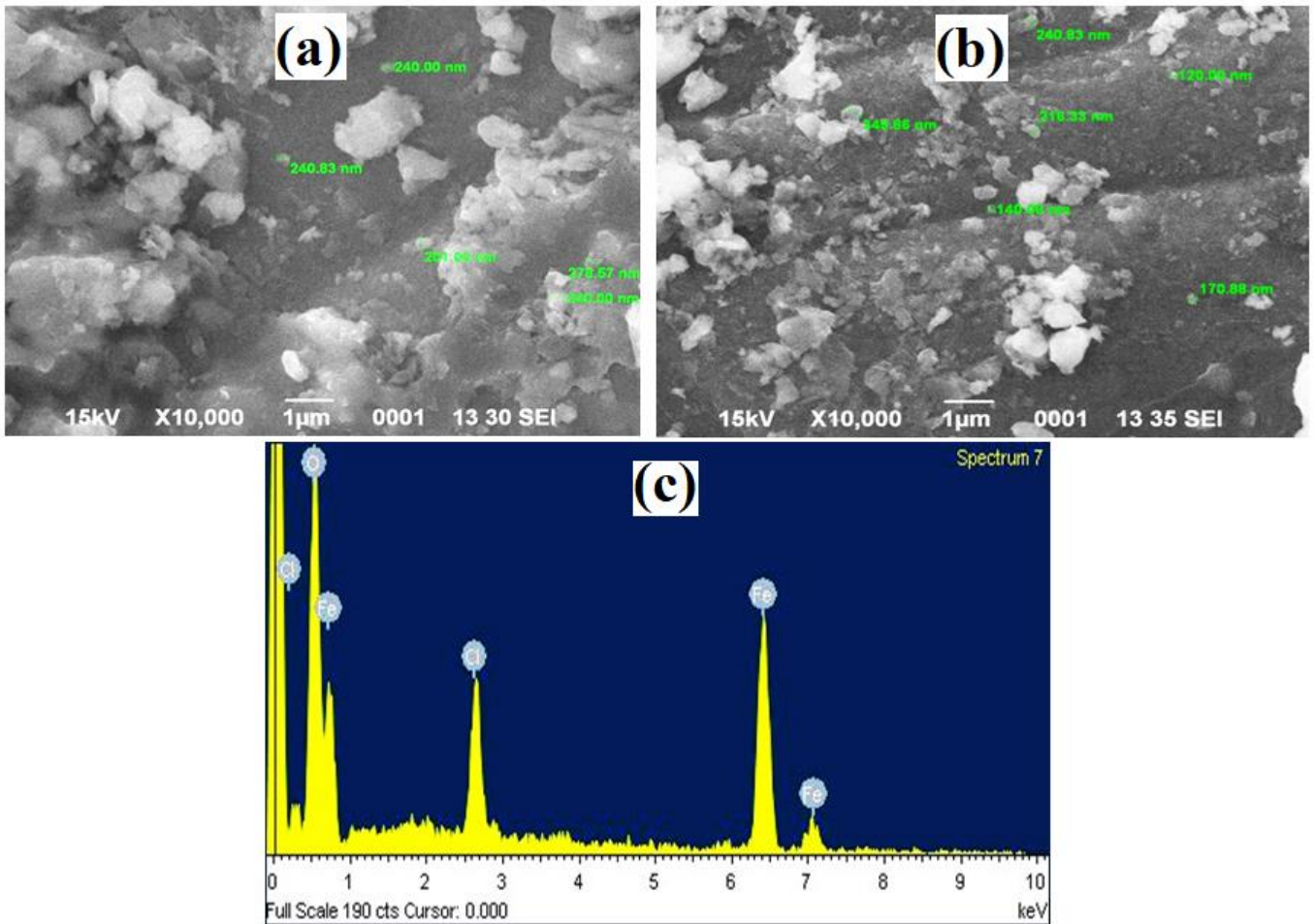


Figure 1. a), b) SEM images of Ca-INPs and c) EDS analysis of Ca-INPs

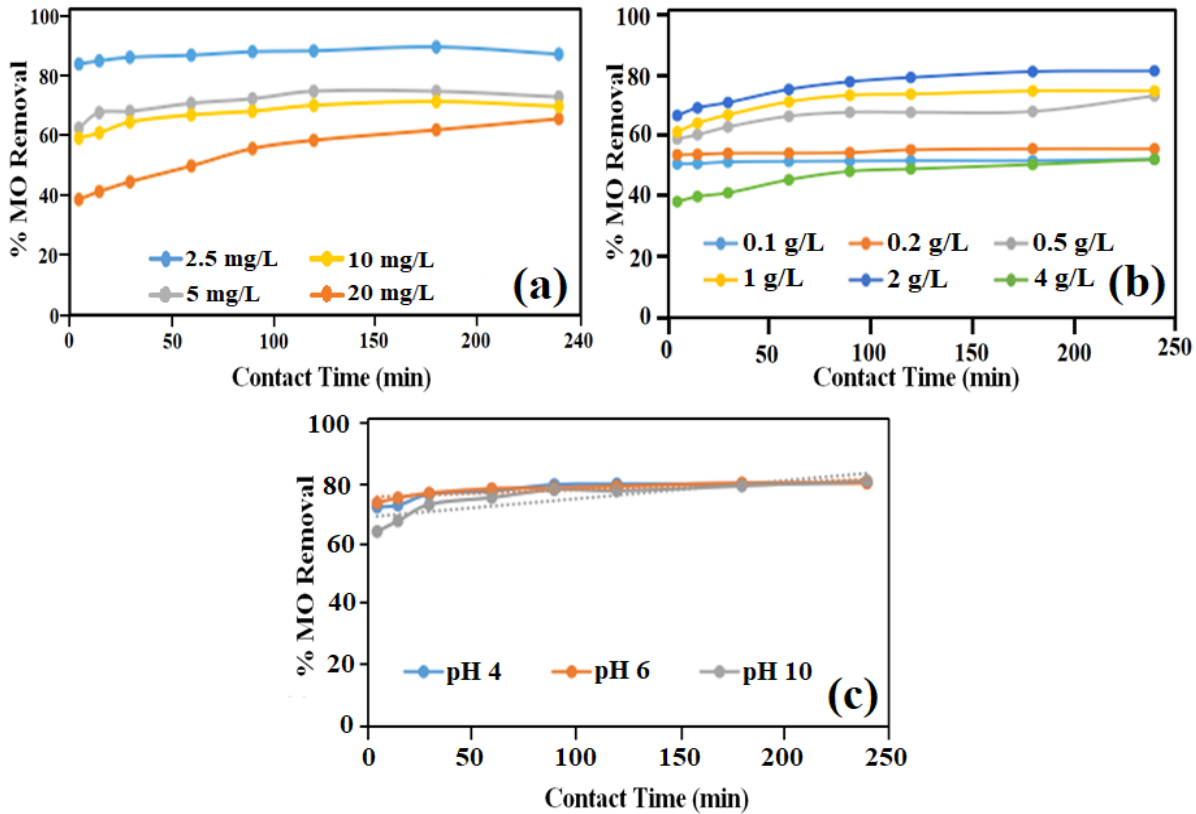


Figure 2. a) Effect of initial MO concentration and contact time, b) effect of Ca-INPs concentration and c) effect of temperature on MO adsorption.

This may result due to increase in number of active sites for adsorption that led more adsorbate molecule to get adsorbed on the nanoparticle surface. And on further increasing Ca-INPs concentration upto 4 g/L the adsorption suddenly drops that may occur due to the agglomeration of nanoparticles in large quantity that increase their particles size and decreased active adsorption sites.

3.3 Effect of contact time and MO concentration

The effect of different MO concentration and varying time contact time were studied at 25°C temperature and at pH 7. The result of the study are represented in Fig. 2a according to which the adsorption of MO was rapid in initial 120 minutes because the active sites were vacant in initial time which facilitated faster uptake of dye molecules by adsorbent, while after 120 min. almost all the active sites get occupied hence the adsorption then get slower at about 120 min equilibrium was reached. On the other hand when MO concentration was increased adsorption of dye was observed to decrease continuously. Highest adsorption 90% was achieved at lowest MO concentration (5 mg/L) and the lowest adsorption was achieved at highest MO concentration (20 mg/L). This occurred because when the concentration of MO was low there were enough active sites for the adsorption of dye molecules present in solution while when the concentration of the dye was increased number of dye molecules increased in the solution whereas, number of active sites was limited due to fix amount of nanoparticles [23][24].

3.4 Effect of pH

pH is an essential parameter to be optimized in adsorption as it is responsible for the charge on adsorbate and adsorbent and governs the degree of ionization and it can also dissociate various functional groups of adsorbent thus it can alter the property of active sites [25]. pH study was done at three different pH values pH 4, pH 6 and pH 10 and results of the study are shown in the Fig. 2c It was observed that adsorption was decreased when the pH of solution was raised upto 10. MO in an anionic dye contains negative charge on it, when pH of the solution increases number of OH⁻ ions also increases in solution these ions competes with dye molecules, this competence between MO molecule and hydroxyl ions results in decrease in dye adsorption. Similar results were reported by Chaari et al, [26] who studied adsorption of anionic dye (Acid Brown 75) onto natural clay.

3.5 Adsorption isotherms

To understand the mechanism behind the adsorption of MO by Ca-INPs Langmuir and Freundlich adsorption isotherm were applied to the adsorption data of MO. Langmuir adsorption isotherm assumes monolayer adsorption of adsorbate on homogenous active sites on the surface of adsorbent. The linear expression of Langmuir isotherm is given below Eq (3) [27]:

$$\frac{C_e}{q_e} = \frac{1}{Q_0 b} + \frac{C_e}{Q_0} \quad (3)$$

Where, C_e and q_e are concentration of MO (mg/L) and amount of MO adsorbed by Ca-INPs (mg/g) at equilibrium

point. Q_0 and b are Langmuir constant that are represents maximum adsorption capacity of Ca-INPs and adsorption rate, respectively. Values of these parameters were derived from the Langmuir isotherm plot between C_e/q_e and C_e (Fig. 3a) R_L which is a dimensionless parameter is also derived in Langmuir isotherm. Value of R_L indicates the favorability of the adsorption process a value greater than one denotes unfavorable adsorption, value equal to one and zero denotes linear and irreversible adsorption, while a R_L value that lies between zero and one represents favorable adsorption process. Value of R_L can be determined by following equation (4):

$$R_L = \frac{1}{1 + bC_0} \quad (4)$$

Freundlich isotherm assumes multilayer adsorption of adsorbate on adsorbent; it describes reversible and non-ideal adsorption process [28]. It suggests that adsorbate will bind on the heterogeneous active sites having different adsorption heat and affinities [29]. Linear equation of Freundlich isotherm is given below in Eq. (5)

$$\ln q_e = \ln K_F \frac{1}{n} \log C_e \quad (5)$$

Where, q_e and C_e are amount of MO adsorbed by Ca-INPs (mg/g) and concentration of MO in solution at equilibrium point, respectively. K_F and n are Freundlich isotherm constant that defines adsorption capacity of Ca-INPs and intensity of MO adsorption, there value was derived by plot between $\ln q_e$ and $\ln C_e$ (Fig. 3b). Values of Langmuir and Freundlich isotherm parameters are shown in the Table 1. On comparing data of both the isotherms, it can be concluded that adsorption of MO was mainly govern by Freundlich isotherm the adsorption was reversible and occurred in multi layers.

Table.1 Values of Langmuir and Freundlich isotherm parameters:

Isotherms	Parameters	Values
Langmuir	Q_0 (mg/g)	21.73
	b (L/mg)	0.145
	R_L	0.0022
	R^2	0.931
Freundlich	K_F (mg/g (L/mg) ^{1/n})	0.0764
	n	0.764
	R_2	0.934

3.6 Adsorption Kinetics

Pseudo-first order and pseudo-second-order kinetic models were applied to the adsorption process; it is helpful in evaluating the mechanism behind the MO adsorption as it gives information about the reaction pathway of adsorption [30]. These kinetics models are helpful in understanding the efficiency of the adsorption process [31]. The linear equations for pseudo-first order and pseudo-second-order kinetics are given below in Eq (6) and Eq (7), respectively:

$$\log(q_e - q_t) = \log q_e - \left(\frac{K_1}{2.303} \right) t \quad (6)$$

$$\frac{t}{q_t} = \frac{1}{K_2 q_e^2} + \frac{1}{q_e} t \quad (7)$$

Where, q_t and q_e are amount of MO adsorbed on Ca-INPs at time t and at equilibrium, respectively. K_1 and K_2 are the pseudo-first-order and pseudo-second-order kinetic rate constants, which were evaluated by the slop and intercept of their respective kinetic model plots (Fig. 3c). The values of both the kinetics parameters are listed in the table 2 which shows that the adsorption data of MO was followed by pseudo-second-order kinetic.

Table 2. Values of pseudo-first and pseudo-second-order kinetic parameters:

C_0 (mg/L)	Pseudo-first-order kinetics			Pseudo-second-order kinetics		
	q_e (mg/g)	k_1 (min ⁻¹)	R^2	q_e (mg/g)	K_2 (g/(mg min))	R^2
2.5	1.09	1.98	0.86	1.09	0.127	0.99
5	1.82	2.02	0.88	1.82	0.086	0.98
10	5.20	1.63	0.81	5.20	0.011	0.99
20	8.8	1.8	0.82	8.8	0.003	0.99

3.7 Intraparticle diffusion model

Weber and Morris [32] proposed an Intraparticle diffusion

model that gives insights of adsorption rate controlling step. The linear expression for Intraparticle diffusion is given below in Eq (8):

$$q_t = K_i t^{1/2} + C_i \quad (8)$$

Where, K_i is the rate of Intraparticle diffusion model ($\text{mg g}^{-1} \text{min}^{-1/2}$) and intercept C_i defines the boundary layer thickness effect. The result of this study is being shown in the Fig. 3d which shows that the straight lines does not crosses the origin (Fig. 3d) which indicates that the Intraparticle diffusion is not the one and only rate controlling step in MO adsorption by Ca-INPs.

4) CONCLUSION

Cauliflower leaf extract was found effective for the synthesis of iron nanoparticles. The nanoparticles were agglomerated as the represented by SEM images. These nanoparticles effectively applied for the removed methyl orange dye from the aqueous solution. The adsorption was decreased when the initial MO concentration was increased upto 20 mg/L. Adsorption was higher in acidic pH which decreased in alkaline pH due to competitive effect of negatively charged hydroxyl radicals. Freundlich isotherm best defined the adsorption of MO with R^2 value 0.9346 that was more than R^2 value (0.9318) of Langmuir

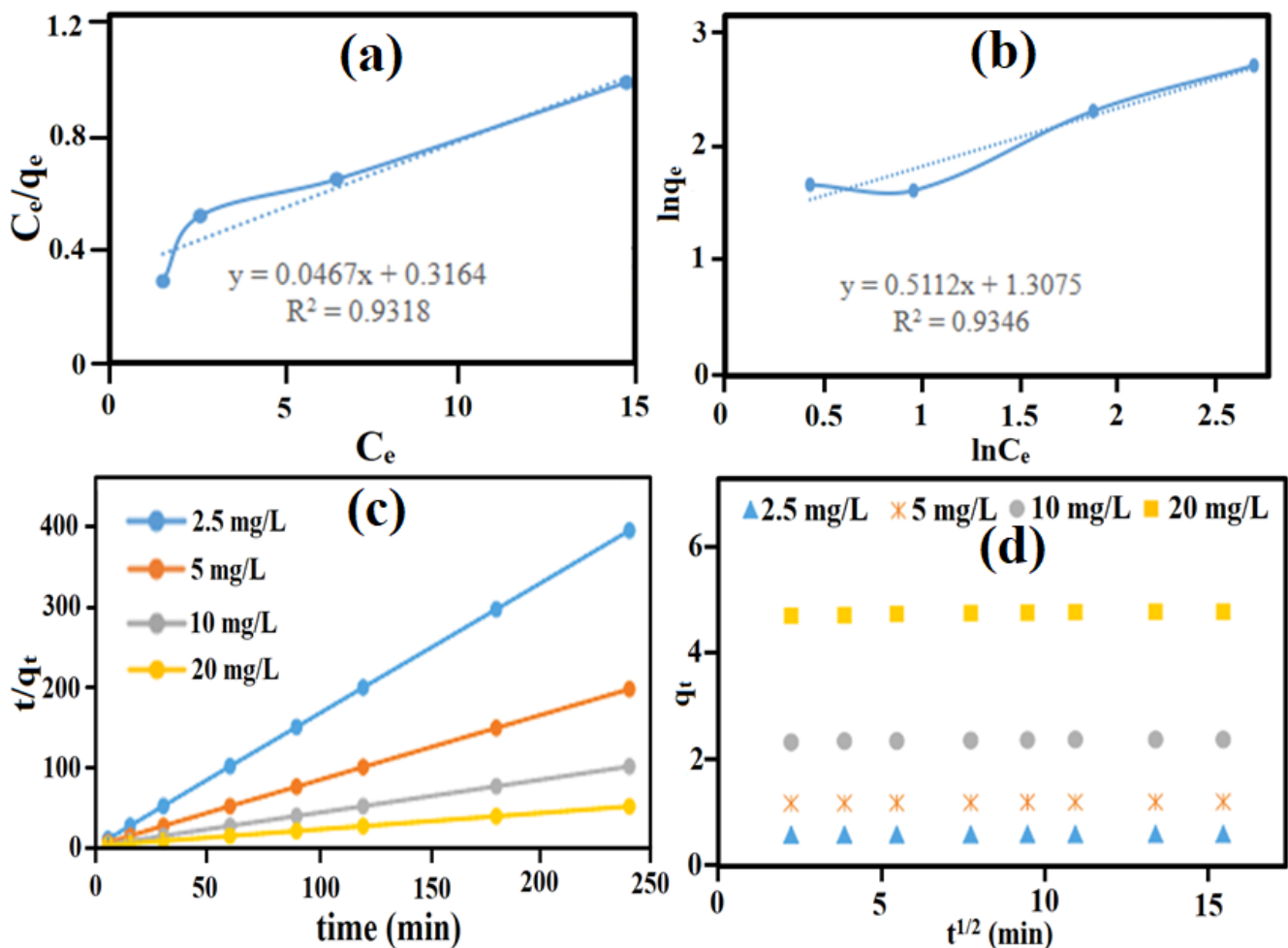


Figure 3. a) Plot for Langmuir isotherm, b) plot for Freundlich isotherm, c) plot for pseudo-second-order kinetic and d) plot for Intraparticle diffusion model.

isotherm. The adsorption process followed pseudo-second-order kinetic with R^2 value closer to one. The adsorption of MO was also analyzed by Intraparticle diffusion model which concluded that Intraparticle diffusion was not the only adsorption limiting factor.

Acknowledgement

University Grant Commission (UGC) of the Government of India (UGC-BSR Research startup grant project No. F. 30-382/2017, BSR), and the Science and Engineering Research Board (SERB), Department of Science and Technology (DST), India, (Reference no. ECR/2016/001924), financially supported the work, hence authors gratefully acknowledge them.

REFERENCES

- 1) Malviya, A., Jaspal, D.K., and Khamparia, S. 2019. Kinetics studies on the adsorption of Methyl Orange and Metanil Yellow onto Bottom Ash: a comparative account. *Water Science and Technology*, 80 (10), 1844–1850.
- 2) Istrate, R., Stoia, M., Păcurariu, C., and Locovei, C. 2019. Single and simultaneous adsorption of methyl orange and phenol onto magnetic iron oxide/carbon nanocomposites. *Arabian Journal of Chemistry*, 12(8), 3704-3722.
- 3) Maneerung, T., Liew, J., Dai, Y., Kawi, S., Chong, C., and Wang, C.H. 2016. Activated carbon derived from carbon residue from biomass gasification and its application for dye adsorption: kinetics, isotherms and thermodynamic studies. *Bioresource technology*, 200, 350-359.
- 4) Deniz, F., and Yildiz, H., 2019. Bioremediation potential of a widespread industrial biowaste as renewable and sustainable biosorbent for synthetic dye pollution. *International journal of phytoremediation*, 21(3), 259-267.
- 5) Lv, S.W., Liu, J.M., Ma, H., Wang, Z.H., Li, C.Y., Zhao, N., and Wang, S. 2019. Simultaneous adsorption of methyl orange and methylene blue from aqueous solution using amino functionalized Zr-based MOFs. *Microporous and Mesoporous Materials*, 282, 179-187.
- 6) Sahu, N., Rawat, S., Singh, J., Karri, R.R., Lee, S., Choi, J.-S., and Koduru, J.R. 2019. Process Optimization and Modeling of Methylene Blue Adsorption Using Zero-Valent Iron Nanoparticles Synthesized from Sweet Lime Pulp. *Applied Science*, 9, 5112.
- 7) Gao, Y., Deng, S.Q., Jin, X., Cai, S.L., Zheng, S.R., and Zhang, W.G. 2019. The construction of amorphous metal-organic cage-based solid for rapid dye adsorption and time-dependent dye separation from water. *Chemical Engineering Journal*, 357, 129-139.
- 8) Darwish, A.A.A., Rashad, M., and AL-Aoh, H.A. 2019. Methyl orange adsorption comparison on nanoparticles: Isotherm, kinetics, and thermodynamic studies. *Dyes and Pigments*, 160, 563-571.
- 9) Borsagli, F.G.M., Ciminelli, V.S., Ladeira, C.L., Haas, D.J., Lage, A.P., and Mansur, H.S. 2019. Multi-functional eco-friendly 3D scaffolds based on N-acyl thiolated chitosan for potential adsorption of methyl orange and antibacterial activity against *Pseudomonas aeruginosa*. *Journal of Environmental Chemical Engineering*, 7(5), 103286.
- 10) Lin, D., Wu, F., Hu, Y., Zhang, T., Liu, C., Hu, Q., Hu, Y., Xue, Z., Han, H., and Ko, T.H. 2020. Adsorption of dye by waste black tea powder: parameters, kinetic, equilibrium, and thermodynamic studies. *Journal of Chemistry*, <https://doi.org/10.1155/2020/5431046>.
- 11) Hasanzadeh, M., Simchi, A., and Far, H.S. 2020. Nanoporous composites of activated carbon-metal organic frameworks for organic dye adsorption: Synthesis, adsorption mechanism and kinetics studies. *Journal of Industrial and Engineering Chemistry*, 81, 405-414.
- 12) Lefebvre, L., Agusti, G., Bouzegane, A., and Edouard, D. 2018. Adsorption of dye with carbon media supported on polyurethane open cell foam. *Catalysis Today*, 301, 98-103.
- 13) Banerjee, S., Dubey S., Gautam, R.K., Chattopadhyaya, M.C., and Sharma, Y.C. 2019. Adsorption characteristics of alumina nanoparticles for the removal of hazardous dye, Orange G from aqueous solutions. *Arabian Journal of Chemistry*, 12(8), 5339-5354.
- 14) Anastopoulos, Ioannis, Ahmad Hosseini-Bandegharaei, Jie Fu, Athanasios C. Mitropoulos, and George Z. Kyzas. "Use of nanoparticles for dye adsorption." *Journal of Dispersion Science and Technology* 39, no. 6 (2018): 836-847.
- 15) Zorro, A., Iannone, A., Natali, S., and Lavecchia, R. 2019. Green synthesis of silver nanoparticles using bilberry and red currant waste extracts. *Processes*, 7(4), 193.
- 16) Vishwasrao, C., Momin, B., and Ananthanarayan, L. 2019. Green synthesis of silver nanoparticles using sapota fruit waste and evaluation of their antimicrobial activity. *Waste and Biomass Valorization*, 10(8), 2353-2363.
- 17) Pan, Z., Lin, Y., Sarkar, B., Owens, G., and Chen, Z. 2019. Green synthesis of iron nanoparticles using red peanut skin extract: Synthesis mechanism, characterization and effect of conditions on chromium removal. *Journal of colloid and interface science*, 558, 106-114.
- 18) Açikel, Ü., Keskin, Z.S., Canbaz, G.T., and Açikel, Y.S. 2019. Synthesis of copper nanoparticles from waste onion peels. *Ispbs-5 Proceedings Book*, 49.
- 19) Dutta, S., Jaiswal, K.K., Verma, R., Basavaraju, D. M., and Ramaswamy, A.P. 2019. Green synthesis of zinc oxide catalyst under microwave irradiation using banana (*Musa spp.*) corm (rhizome) extract for biodiesel synthesis from fish waste lipid. *Biocatalysis and Agricultural Biotechnology*, 22, 101390.
- 20) Lingamdinne, L.P., Chang, Y.-Y., Yang, J.-K., Singh, J., Choi, E.-H., Shiratani, M., Koduru, J.R., and Attri, P. 2017. Biogenic reductive preparation of magnetic inverse spinel iron oxide nanoparticles for the adsorption removal of heavy metals. *Chemical Engineering Journal*, 307, 74-84.
- 21) Devatha, C.P., Thalla, A.K., and Katte, S.Y. 2016. Green synthesis of iron nanoparticles using different leaf

- extracts for treatment of domestic waste water. *Journal of cleaner production*, 139, 1425-1435.
- 22) Molla Mahmoudi, M., Nadali, A., Soheil, A.H.R., and Mahvi, A.H. 2019. Adsorption of cationic dye textile wastewater using Clinoptilolite: isotherm and kinetic study. *The journal of the Textile Institute*, 110(1), 74-80.
 - 23) Mishra, S., Yadav, S.S., Rawat, S., Singh, J., and Koduru, J.R. 2019. Corn husk derived magnetized activated carbon for the removal of phenol and para-nitrophenol from aqueous solution: Interaction mechanism, insights on adsorbent characteristics, and isothermal, kinetic and thermodynamic properties. *Journal of Environmental Management*, 246, 362-373.
 - 24) Yadav, N., Maddheshiaya, D.N., Rawat, S., and Singh, J. 2020. Adsorption and equilibrium studies of phenol and para-nitrophenol by magnetic activated carbon synthesised from cauliflower waste. *Environmental Engineering Research*, 25(5), 742-752.
 - 25) Banerjee, S., and Chattopadhyaya, M.C. 2017. Adsorption characteristics for the removal of a toxic dye, tartrazine from aqueous solutions by a low cost agricultural by-product. *Arabian Journal of Chemistry*, 10(2), 1629-1638.
 - 26) Chaari, I., Fakhfakh, E., Medhioub, M., and Jamoussi, F. 2019. Comparative study on adsorption of cationic and anionic dyes by smectite rich natural clays. *Journal of Molecular Structure*, 1179, 672-677.
 - 27) Gautam, A., Rawat, S., Verma, L., Singh, J., Sikarwar, S., Yadav, B.C., and Kalamdhad, A.S. 2018. Green synthesis of iron nanoparticle from extract of waste tea: An application for phenol red removal from aqueous solution. *Environmental Nanotechnology, Monitoring & Management*, 10, 377-387.
 - 28) Ibrahim, M., Siddique, A., Verma, L., Singh, J., and Koduru, J.R. 2019. Adsorptive Removal of Fluoride from Aqueous Solution by Biogenic Iron Permeated Activated Carbon Derived from Sweet Lime Waste. *Acta Chimica Slovenica*, 66, 123-136.
 - 29) Kumar, P.S., Korving, L., Keesman, K. J., van Loosdrecht, M.C., and Witkamp, G. J. 2019. Effect of pore size distribution and particle size of porous metal oxides on phosphate adsorption capacity and kinetics. *Chemical Engineering Journal*, 358, 160-169.
 - 30) Pholosi, A., Naidoo, E.B., and Ofomaja, A.E. 2020. Intraparticle diffusion of Cr (VI) through biomass and magnetite coated biomass: A comparative kinetic and diffusion study. *South African Journal of Chemical Engineering*, 32, 39-55.
 - 31) Naushad, M., Ahamad, T., AlOthman, Z.A., and Ala'a, H. 2019. Green and eco-friendly nanocomposite for the removal of toxic Hg (II) metal ion from aqueous environment: adsorption kinetics & isotherm modelling. *Journal of Molecular Liquids*, 279, 1-8.
 - 32) Weber, W.J., and Morris, J.C. 1963. Kinetics of adsorption on carbon from solution. *Journal of the sanitary engineering division*, 89(2), 31-60.